Progress In Electromagnetics Research, *PIER 28, 205–229, 2000*

ANALYSIS OF RECTANGULAR WAVEGUIDE H-PLANE JUNCTIONS IN NONORTHOGONAL COORDINATE SYSTEM

R. Dusséaux

CETP-IPSL, CNRS-UVSQ
Université de Versailles Saint-Quentin en Yvelines
10/12 Avenue de l'Europe, 78140 Vélizy, France

P. Chambelin

Alcatel
26 Avenue Champollion
31037 Toulouse, France

C. Faure

LASMEA, Université Blaise Pascal
24 Avenue des Landais, BP 45
63177 Aubière, France

1. Introduction
2. Propagation Equations
2.1 Tensorial Covariant Formalism of Maxwell's Equations
2.2 Coordinate System – Metric Tensor
2.3 Fields Components Inside the Junction and Rectangular Waveguides
2.4 Continuity of Field and Boundary Conditions
3. Multimodal Scattering Matrix
3.1 Initial Value Problem
3.2 Discontinuities with a Longitudinal Symmetry Plane
3.3 Initial Vectors and Generalized Scattering Matrix
4. Numerical Results
4.1 Restrictions of Numerical Nature

4.2 Analysis of a Sinusoidal Profile Filter
4.3 Steep Discontinuities and Adapted Sectoral Horn
5. Conclusion
References

1. INTRODUCTION

In this paper, we look at the scattering behavior of different H-plane discontinuities in rectangular waveguides (tapers, filters, adapted sectoral horns). These components are translationally symmetric along one of two transverse directions. An H-plane discontinuity presents an incident electric field parallel to the unchanged transverse direction. Such a junction excited by a TE_{n0} generates modes of the same nature in access rectangular waveguides [1]. The generalized modal scattering matrix relates outgoing TE_{n0} modes to incoming TE_{n0} modes. Our main purpose is to define this matrix by taking into account propagating and evanescent waves.

For this purpose, Maxwell's equations are used in tensorial form, written in a nonorthogonal coordinate system where the boundary surfaces coincide with coordinate surfaces [2]. As a result, the expression of boundary conditions on the perfectly conducting walls becomes simplified. The complexity is transferred to the analytical expression of propagation equations [2, Chap. 2]. This formalism have given rise to some works in waveguide field. The first studies consider periodic waveguides with axial revolution symmetry [3, 4]. Those that follow have been interested in H-plane and E-plane discontinuities: waveguide bent [5–7] and tapers [8–10].

The nonorthogonal curvilinear coordinate formalism is briefly described in Section 2. This formalism uses the covariant components E_i and H_i of electric and magnetic fields, respectively. These components inside the junction fulfill a differential system with non-constant coefficients. This system becomes identified with an initial value problem [9, 10]. Its numerical integration with many independent initial vectors (independent combinations of eigenmodes TE_{n0}) allows the generalized modal scattering matrix to be obtained. The solving and integration principles presented in [9] are fitted to specifics of H-plane discontinuities (Section 3). Moreover, in this paper, we prove that to obtain a $2N \times 2N$-dimensional scattering matrix, it is only necessary to do N numerical integrations and not $2N$. With respect to previous works [5, 6, 8–10], the gain in computation time is then of 2.

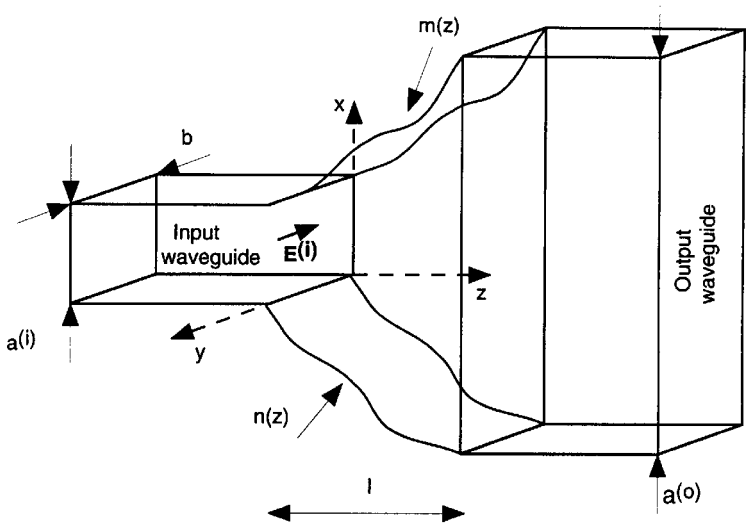

Figure 1. H-plane taper. Size b with respect to the Oy axis is constant. Functions $m(z)$ and $n(z)$ that describe the structure walls can be different. Incident field $\vec{E}^{(i)}$ is parallel to the Oy axis.

In this paper, we take a special interest in H-plane discontinuities with a longitudinal symmetry. With this nonorthogonal curvilinear coordinate formalism, propagation equations contain the problem geometry. The initial value system contains then the junction symmetries and the electromagnetic consequences can easily be deduced. In particular, an odd mode $TE_{2n+1,0}$ incident upon an H-plane discontinuity with a longitudinal symmetry only excites odd modes TE in rectangular waveguides. A similar conclusion is obtained in the case of even modes. A new demonstration that confirms this well-known physical result is here proposed.

In Section 4, a structure with two septums is analyzed on the range 8–16 GHz , then on an adapted sectoral horn and finally on a sinusoidal profile filter on 10–15 GHz . Several results are presented. The theory is verified by comparison with results obtained by other methods [11–13].

2. PROPAGATION EQUATIONS

2.1 Tensorial Covariant Formalism of Maxwell's Equations

The studied H-plane junction in Figure 1 is a length l microwave component that ensures the continuity between two rectangular waveguides with different sizes. Input and output waveguides are of cross section $a^{(i)} \times b$ and $a^{(o)} \times b$, respectively. (Afterwards, letters $(g) = (i)$ and $(g) = (o)$ denote quantities relative to input and output waveguides, respectively). Functions $x = m(z)$ and $x = n(z)$ that describe the perfectly conducting walls can be different. It is assumed that higher modes can propagate in rectangular waveguides and the dominant mode TE_{10} is incident upon the junction.

We choose to solve the electromagnetic problem in a nonorthogonal coordinate system fitted to the studied component geometry. In a curvilinear coordinate system (x^1, x^2, x^3), the Maxwell equations [2, Chap. 1] are given by (1):

$$\begin{aligned} \frac{1}{\sqrt{g}}\left(\frac{\partial E_k}{\partial x^j} - \frac{\partial E_j}{\partial x^k}\right) &= -\frac{\partial B^i}{\partial t} \qquad (i,j,k) = (1,2,3); \\ \frac{1}{\sqrt{g}}\left(\frac{\partial H_k}{\partial x^j} - \frac{\partial H_j}{\partial x^k}\right) &= \frac{\partial D^i}{\partial t} + J^i \qquad\quad (2,3,1); \\ & \qquad\qquad\qquad\qquad\quad (3,1,2) \end{aligned} \tag{1a}$$

$$\begin{aligned} \frac{1}{\sqrt{g}}\sum_{i=1}^{3}\frac{\partial(\sqrt{g}D^i)}{\partial x^i} &= \rho \\ \frac{1}{\sqrt{g}}\sum_{i=1}^{3}\frac{\partial(\sqrt{g}B^i)}{\partial x^i} &= 0 \end{aligned} \tag{1b}$$

E_i and H_i are the covariant components of electric vector $\mathbf{E}$ and magnetic vector $\mathbf{H}$. D^i, B^i, and J^i are the contravariant components of vectors electric displacement $\mathbf{D}$, magnetic induction $\mathbf{B}$ and current density $\mathbf{J}$, respectively. ρ is the charge density. g is the determinant of metric tensor.

For a homogeneous and isotropic medium with permittivity ε_0 and permeability μ_0 the Maxwell equations (1) must be associated with the medium relations (2):

$$D^i = \varepsilon_0 E^i = \varepsilon_0 \sum_{j=1}^{3} g^{ij} E_j; \qquad B^i = \mu_0 H^i = \mu_0 \sum_{j=1}^{3} g^{ij} H_j \tag{2}$$

If there is no current density and no charge density, then Maxwell equations (1) and medium relations (2) expressed in a general coordinate system (x^1, x^2, x^3) lead to set of 6 partial differential equations relating the covariant components E_i and H_i. The time factor is in $\exp(j\omega t)$ where ω is the angular frequency.

$$\begin{aligned} &\frac{\partial E_k}{\partial x^j} - \frac{\partial E_j}{\partial x^k} = -jk\sqrt{g}g^{ij}ZH_j \\ &\frac{\partial H_k}{\partial x^j} - \frac{\partial H_j}{\partial x^k} = jk\sqrt{g}g^{ij}E_j \\ &Z = \sqrt{\mu_0/\varepsilon_0}; \quad k = 2\pi/\lambda \end{aligned} \qquad (i,j,k) = (1,2,3); (2,3,1); (3,1,2) \tag{3}$$

2.2 Coordinate System – Metric Tensor

The nonorthogonal coordinate system (u, v, w) fitted to the junction geometry is obtained from the Cartesian system (x, y, z) by the transformation (4):

$$\begin{aligned} u &= a^{(i)} \frac{x - n(z)}{m(z) - n(z)} \\ v &= y \\ w &= z \end{aligned} \tag{4}$$

In this new coordinate system, the waveguide walls coincide with the following coordinate surfaces:

$$\begin{aligned} x = n(z) \quad &\Leftrightarrow \quad u = 0 \\ x = m(z) \quad &\Leftrightarrow \quad u = a^{(i)} \end{aligned} \tag{5}$$

The change from Cartesian components (t_x, t_y, t_z) of vector $\mathbf{t}$ to covariant components (t_u, t_v, t_w) is given by:

$$\begin{pmatrix} t_u \\ t_v \\ t_w \end{pmatrix} = \mathbf{A} \begin{pmatrix} t_x \\ t_y \\ t_z \end{pmatrix} \tag{6}$$

where $\mathbf{A}$ denotes the Jacobian transformation matrix (7):

$$\mathbf{A} = \begin{pmatrix} A_u^x & A_u^y & A_u^z \\ A_v^x & A_v^y & A_v^z \\ A_w^x & A_w^y & A_w^z \end{pmatrix} = \begin{pmatrix} \frac{\partial x}{\partial u} & \frac{\partial y}{\partial u} & \frac{\partial z}{\partial u} \\ \frac{\partial x}{\partial v} & \frac{\partial y}{\partial v} & \frac{\partial z}{\partial v} \\ \frac{\partial x}{\partial w} & \frac{\partial y}{\partial w} & \frac{\partial z}{\partial w} \end{pmatrix}$$

$$= \begin{pmatrix} \dfrac{h(z)}{a^{(i)}} & 0 & 0 \\ 0 & 1 & 0 \\ u\dfrac{h'(z)}{a^{(i)}} + n'(z) & 0 & 1 \end{pmatrix} \tag{7a}$$

$$h(z) = m(z) - n(z); \qquad h'(z) = \frac{dh(z)}{dz} = m'(z) - n'(z) \tag{7b}$$

The covariant component t_v becomes identified with t_y. Moreover, the covariant component t_w is parallel to the waveguide walls given by $u = 0$ and $u = a^{(i)}$ (8):

$$\begin{aligned} t_u &= \frac{h(z)}{a^{(i)}} t_x \\ t_v &= t_y \\ t_w &= \frac{\left(uh'(z) + a^{(i)} n'(z)\right)}{a^{(i)}} t_x + t_z \end{aligned} \tag{8}$$

The change (9) from covariant components (t_u, t_v, t_w) to contravariant (t^u, t^v, t^w) is obtained by the metric tensor $\mathbf{G}$ (10).

$$\begin{pmatrix} t_u \\ t_v \\ t_w \end{pmatrix} = \mathbf{G} \begin{pmatrix} t^u \\ t^v \\ t^w \end{pmatrix} \quad \Leftrightarrow \begin{pmatrix} t^u \\ t^v \\ t^w \end{pmatrix} = \mathbf{G}^{-1} \begin{pmatrix} t_u \\ t_v \\ t_w \end{pmatrix} \tag{9}$$

The tensor metric $\mathbf{G_c}$ associated with Cartesian system is the identity matrix. $\mathbf{A^t}$ denotes the adjoint matrix of $\mathbf{A}$. The $\mathbf{G}$ determinant (10c) is a strictly positive z-function.

$$\mathbf{G} = \mathbf{A}\mathbf{G_c}\mathbf{A^t} = \begin{pmatrix} g_{uu} & g_{uv} & g_{uw} \\ g_{vu} & g_{vv} & g_{vw} \\ g_{wu} & g_{wv} & g_{ww} \end{pmatrix}$$

$$= \begin{pmatrix} \left(\dfrac{h(z)}{a^{(i)}}\right)^2 & 0 & \dfrac{h(z)}{a^{(i)}}\left(\dfrac{uh'(z)}{a^{(i)}} + n'(z)\right) \\ 0 & 1 & 0 \\ \dfrac{h(z)}{a^{(i)}}\left(\dfrac{uh'(z)}{a^{(i)}} + n'(z)\right) & 0 & \left(\dfrac{uh'(z)}{a^{(i)}} + n'(z)\right)^2 + 1 \end{pmatrix} \tag{10a}$$

$$
\begin{aligned}
&\mathbf{G}^{-1} \\
&= \begin{pmatrix} g^{uu} & g^{uv} & g^{uw} \\ g^{vu} & g^{vv} & g^{vw} \\ g^{wu} & g^{wv} & g^{ww} \end{pmatrix} \\
&= \begin{pmatrix} \dfrac{\left(uh'(z)+a^{(i)}n'(z)\right)^2 + a^{(i)2}}{h(z)^2} & 0 & -\dfrac{uh'(z)+a^{(i)}n'(z)}{h(z)} \\ 0 & 1 & 0 \\ -\dfrac{uh'(z)+a^{(i)}n'(z)}{h(z)} & 0 & 1 \end{pmatrix} \qquad (10b) \\
&g = \left(\frac{h(z)}{a^{(i)}}\right)^2 \qquad (10c)
\end{aligned}
$$

The expression (11) of contravariant components in terms of Cartesian ones is obtained from (8, 9) and (10b). We note that the field component t^u is normal to coordinate surfaces $u = 0$ and $u = a^{(i)}$.

$$
\begin{aligned}
t^u &= \frac{1}{h(z)}\left(a^{(i)}t_x - (uh' + a^{(i)}n't_z\right) \\
t^v &= t_y \\
t^w &= t_z
\end{aligned} \qquad (11)
$$

2.3 Fields Components Inside the Junction and Rectangular Waveguides

There is no incident field and structural variation in the y coordinate, so we can write:

$$\frac{\partial}{\partial y} = \frac{\partial}{\partial v} = 0 \qquad (12)$$

Substituting (10b) and (12) in (3), we obtain the expression of E_u, H_u, E_w, and H_w in terms of E_v and H_v only:

$$
\begin{aligned}
ZH_u &= \frac{1}{k^2}\left(-jk\sqrt{g}g^{zz}\frac{\partial E_v}{\partial z} - jk\sqrt{g}g^{zu}\frac{\partial E_v}{\partial u}\right) \\
ZH_w &= \frac{1}{k^2}\left(jk\sqrt{g}g^{zu}\frac{\partial E_v}{\partial z} + jk\sqrt{g}g^{uu}\frac{\partial E_v}{\partial u}\right) \\
E_u &= \frac{1}{k^2}\left(jk\sqrt{g}g^{zz}\frac{\partial ZH_v}{\partial z} + jk\sqrt{g}g^{zu}\frac{\partial ZH_v}{\partial u}\right) \\
E_w &= \frac{1}{k^2}\left(-jk\sqrt{g}g^{zu}\frac{\partial ZH_v}{\partial z} - jk\sqrt{g}g^{uu}\frac{\partial ZH_v}{\partial u}\right)
\end{aligned} \qquad (13)
$$

and we can express independent propagation equations for $E_y = E_v$ and $H_y = H_v$:

$$\partial_u\left(\sqrt{g}\left(g^{uu}\partial_u E_v + g^{uz}\partial_z E_v\right)\right) + \partial_z\left(\sqrt{g}\left(g^{zu}\partial_u E_v + g^{uz}\partial_z E_v\right)\right) + \sqrt{g}k^2 E_v = 0 \tag{14a}$$

$$\partial_u\left(\sqrt{g}\left(g^{uu}\partial_u H_v + g^{uz}\partial_z H_v\right)\right) + \partial_z\left(\sqrt{g}\left(g^{zu}\partial_u H_v + g^{uz}\partial_z H_v\right)\right) + \sqrt{g}k^2 H_v = 0 \tag{14b}$$

According to (8), (13), and (14), an H-plane discontinuity that is excited by the dominant mode TE_{10} (expression (15) with $n = 0$, $H_y^{(i)} = 0$) only can generate 3 covariant components H_u, H_w, and E_v ($E_u = E_w = H_v = 0$). A similar conclusion can be obtained if the incident mode is of the type TE_{n0} (15). Therefore, the reflected and transmitted fields in rectangular waveguides are given by linear combinations of independent modes TE_{n0}.

$$E_y^{(g)}(x,z) = \sum_{n=1}^{+\infty}\left(W_n^{(g+)}\exp(-j\gamma_{n0}z) + W_n^{(g-)}\exp(+j\gamma_{n0}z)\right)\sin\left(\frac{n\pi x}{a^{(g)}}\right) \tag{15a}$$

$$H_x^{(g)}(x,z) = \sum_{n=1}^{+\infty}\left(Y_n^{(g+)}\exp(-j\gamma_{n0}z) + Y_n^{(g-)}\exp(+j\gamma_{n0}z)\right)\sin\left(\frac{n\pi x}{a^{(g)}}\right) \tag{15b}$$

$$E_x^{(g)} = E_z^{(g)} = 0; \quad H_y^{(g)} = 0; \quad H_z^{(g)} = \frac{-1}{jkZ}\frac{\partial E_y}{\partial x} \tag{15c}$$

The quantities $W_n^{(g\pm)}$ and $Y_n^{(g\pm)}$ are linked by the impedance $Z_n^{(g)}$ (16).

$$Y_n^{(g+)} = -\frac{W_n^{(g+)}}{Z_n^{(g)}}, \quad Y_n^{(g-)} = \frac{W_n^{(g-)}}{Z_n^{(g)}}, \quad Z_n^{(g)} = \frac{kZ}{\gamma_{n0}^{(g)}} \tag{16}$$

The constant propagation $\gamma_{n0}^{(g)}$ defines the nature of wave (17):

$$\begin{aligned} &\gamma_{n0}^{(g)} \text{ is real for a propagating mode}: \gamma_{n0}^{(g)} = \sqrt{k^2 - \left(\frac{n\pi}{a^{(g)}}\right)^2} \\ &\gamma_{n0}^{(g)} \text{ is imaginary for a evanescent mode}: \gamma_{n0}^{(g)} = -j\sqrt{\left(\frac{n\pi}{a^{(g)}}\right)^2 - k^2} \end{aligned} \tag{17}$$

The normalized amplitude coefficients $\left(A_n^{(g)}; B_n^{(g)}\right)$ associated with mode TE_{n0} are defined by expressions (17). With this definition, $A_n^{(g)}$ is associated with a wave moving in direction $+z$, $B_n^{(g)}$ in direction $-z$, respectively.

$$A_n^{(g)} = \frac{W_n^{(g+)}}{\sqrt{Z_n^{(g)}}} \exp\left(-j\gamma_{n0}^{(g)} z\right); \quad B_n^{(g)} = \frac{W_n^{(g-)}}{\sqrt{Z_n^{(g)}}} \exp\left(+j\gamma_{n0}^{(g)} z\right) \tag{18}$$

2.4 Continuity of Field and Boundary Conditions

In accordance with (8), continuity of field transverse components in planes $z = 0$ and $z = l$ is given as follows:

$$\text{in } z = 0, \quad H_x^{(i)}(x,z) = H_u(u,z) \quad \text{with } u = x \tag{19a}$$
$$E_y^{(i)}(x,z) = E_v(u,z)$$
$$\text{in } z = l, \quad H_x^{(o)}(x,z) = \frac{a^{(o)}}{a^{(i)}} H_u(u,z) \quad \text{with } u = (x - n(l))/a^{(o)} \tag{19b}$$
$$E_y^{(0)}(x,z) = E_v(u,z)$$

These relations lead us to study the propagation of covariant components $H_u(u,z)$ and $E_v(u,z)$ inside the structure.

The electric component $E_v(u,z)$ is parallel to perfectly conducting walls. $E_v(u,z)$ is zero in $u = 0$ and $u = a^{(i)}$. The function $E_v(u,z)$ is then expanded on $\sin(\alpha_n u)$ basis functions with $\alpha_n = n\pi/a^{(i)}$ (20).

$$e_v(u,z) = \sum_{n=1}^{+\infty} V_n(z) \sin(\alpha_n u) \tag{20}$$

In most cases, the magnetic component $H_u(u,z)$ is not normal to waveguide walls. Thus, $H_u(u,z)$ is non-zero in $u = 0$ and $u = a^{(i)}$ ($H_u(u,z) = 0$ in $u = 0$ or $u = a^{(i)}$ if and only if $n'(z) = 0$ or $m'(z) = 0$, respectively). In accordance with (15b), $H_x^{(g)}(x,z)$ is expressed as $\sin(n\pi x/a^{(g)})$ basis functions. In order to make the solving of field continuity relations (19) easier, $H_u(u,z)$ is also expanded as $\sin(\alpha_n u)$ basis functions (21).

$$h_u(u,z) = \sum_{n=0}^{+\infty} I_n(z) \sin(\alpha_n u) \tag{21}$$

The restriction of Fourier series $e_v(u,z)$ on $[0;a^{(i)}]$ expresses the distribution of $E_v(u,z)$ on this same interval. But, $H_u(u,z)$ is equal to $h_u(u,z)$ only on the interval $]0;a^{(i)}[$. For any H-plane discontinuity, the second magnetic component $H_z(u,z) = H_w(u,z)$ is tangential to boundary surfaces. $H_w(u,z)$ is non-zero in $u = 0$ and $u = a^{(i)}$, hence:

$$h_w(u,z) = \sum_{n=0}^{+\infty} H_n(z)\cos(\alpha_n u); \quad H_w(u,z) = h_w(u,z)\text{on}\left[0;a^{(i)}\right] \tag{22}$$

3. MULTIMODAL SCATTERING MATRIX

3.1 Initial Value Problem

Combining (13) and (14), we obtain differential system (23):

$$\frac{\partial E_v}{\partial z} = D(u,z)\frac{\partial E_v}{\partial u} + jkC(z)ZH_u \tag{23a}$$

$$\frac{\partial H_u}{\partial z} = \frac{\partial H_w}{\partial u} + \frac{jk}{ZC(z)}E_v \tag{23b}$$

with

$$ZH_w = \frac{-1}{jk}C(z)\frac{\partial E_v}{\partial u} + D(u,z)H_u \tag{24}$$

$$D(u,z) = -\frac{g^{zu}}{g^{zz}} = \frac{uh'(z) + a^{(i)}n'(z)}{h(z)} \tag{25a}$$

$$C(z) = \frac{1}{\sqrt{g}g^{zz}} = \frac{a^{(i)}}{h(z)} \tag{25b}$$

$e_v(u,z)$, $h_u(u,z)$, and $h_w(u,z)$ are of period $2a^{(i)}$. $e_v(u,z)$ and $h_w(u,z)$ are continuous and at least once differentiable functions in terms of u. Their derivatives $\frac{\partial e_v}{\partial u}$ and $\frac{\partial h_w}{\partial u}$ becomes identified with derivatives of expansions in Fourier series. Substituting geometric function $D(u,z)$ with its expansion in sinus series (26), $e_v(u,z)$, $h_u(u,z)$, and $h_w(u,z)$ are solutions of (23) and (24). With this expansion (26), left and right-hand sides of (23) are both odd functions in terms of u

and left and right-hand sides of (24) are both even.

$$\begin{aligned} d(u,z) &= \sum_{q=0}^{+\infty} d_q(z)\sin(\alpha_q u); \quad D(u,z) = d(u,z)\text{on}\left[0; a^{(i)}\right] \\ d_{q>0}(z) &= \frac{1}{\alpha_q h(z)}\left((-1)^q m'(z) + n'(z)\right); \quad d_0(z) = 0. \end{aligned} \tag{26}$$

Finally, after projecting (23) and (24) on trigonometric functions, several elementary calculations lead to a set of partial differential equations (27) relating the coefficients $V_n(z)$ and $I_n(z)$. This system becomes identified with an initial value problem [14]. The fourth order Runge Kutta method is chosen for numerical integrations from $z = 0$ to $z = l$.

$$\frac{\partial V_n}{\partial z} = \sum_{q=1}^{+\infty} \left(d_{q+n} - d_{q-n}\right)\alpha_q V_q + jkZI_n \tag{27a}$$

$$\frac{\partial I_n}{\partial z} = \left(\frac{C(z)}{jkZ}\alpha_n^2 + \frac{jk}{ZC(z)}\right)V_n - \alpha_n \sum_{q=1}^{+\infty}\left(d_{q+n} + d_{q-n}\right)I_q \tag{27b}$$

The numerical solution of (27) requires a truncation order N. It is then assumed that fields components E_v and H_u are well described by only N coefficients $V_n(z)$ and $I_n(z)$ (in (20, 21), $V_{n>N}(z) = I_{n>N}(z) = 0$).

3.2 Discontinuities with a Longitudinal Symmetry Plane

Such a discontinuity has the symmetry plane $x = \frac{a^{(i)}}{2}$. Thus, coefficients d_n are even and are given as follows:

$$\begin{aligned} m(z) &= a^{(i)} - n(z) \\ d_{2q}(z) &= \frac{2n'(z)}{\alpha_{2q}\left(a^{(i)} - 2n(z)\right)} \quad \text{and} \quad d_{2q+1}(z) = 0 \end{aligned} \tag{28}$$

In accordance with (28), we prove that odd amplitudes (V_{2n+1}, I_{2n+1}) and even amplitudes (V_{2n}, I_{2n}) fulfill two sets of non-coupled differential equations (29) and (30), respectively:

$$\frac{\partial V_{2n+1}}{\partial z} = \sum_{q=0}^{+\infty}\left(d_{2(q+n+1)} - d_{2(q-n)}\right)\alpha_{2q+1}V_{2q+1} + jkZI_{2n+1} \tag{29a}$$

$$\frac{\partial I_{2n+1}}{\partial z} = \left(\frac{C(z)}{jkZ}\alpha_{2n+1}^2 + \frac{jk}{ZC(z)}\right) V_{2n+1} - \alpha_{2n+1} \sum_{q=0}^{+\infty} \left(d_{2(q+n+1)} + d_{2(q-n)}\right) I_{2q+1} \tag{29b}$$

and

$$\frac{\partial V_{2n}}{\partial z} = \sum_{q=1}^{+\infty} \left(d_{2(q+n)} - d_{2(q-n)}\right) \alpha_{2q} V_{2q} + jkZI_{2n} \tag{30a}$$

$$\frac{\partial I_{2n}}{\partial z} = \left(\frac{C(z)}{jkZ}\alpha_{2n}^2 + \frac{jk}{ZC(z)}\right) V_{2n} - \alpha_{2n} \sum_{q=1}^{+\infty} \left(d_{2(q+n)} + d_{2(q-n)}\right) V_q \tag{30b}$$

Consequently, an odd mode $TE_{2n+1,0}$ incident upon an H-plane discontinuity with a longitudinal symmetry only excites odd modes TE in rectangular waveguides. A similar conclusion is obtained in the case of even modes. With this nonorthogonal curvilinear coordinate formalism, propagation equations contain the problem geometry. The initial value system contains then the structure symmetries and thus the electromagnetic consequences can easily be deduced. This is an indisputable advantage of this method.

3.3 Initial Vectors and Generalized Scattering Matrix

Pairs (V_n, I_n) and $(V_n^*, -I_n^*)$ fulfill the same differential system (27) (h^* designates the complex conjugate of h). Taking into account this remark, we prove that a $2N \times 2N$ scattering matrix is obtained with only N numerical integrations instead of $2N$. With respect to previous works [5, 6, 8–10], the gain in computation time is then of 2.

First, N independent vectors putting together normalized amplitudes $\left(A_1^{(i)}, A_2^{(i)}, \ldots, A_N^{(i)}, B_1^{(i)}, B_2^{(i)}, \ldots, B_N^{(i)}\right)_m$ are defined as follows:

For a propagating mode:

$$\forall n, m \in [1, N], \quad \left(A_n^{(i)}\right)_m = K_n \delta_{n,m}; \quad \left(B_n^{(i)}\right)_m = 0; \quad \left(P_n^{(i)}\right)_m = \delta_{n,m} \tag{31a}$$

For an evanescent mode:

$$\forall n, m \in [1, N], \quad \left(A_n^{(i)}\right)_m = K_n \delta_{n,m}; \quad \left(B_n^{(i)}\right)_m = \frac{-jK_n}{2}\delta_{n,m}; \quad \left(P_n^{(i)}\right)_m = \delta_{n,m} \tag{31b}$$

$\delta_{n,m}$ denotes the Kronecker symbol. $K_n = \frac{2}{\sqrt{a^{(i)}b}}$ is a normalization constant, so that the power carried $\left(P_n^{(i)}\right)_n$ by a given mode TE_{n0} into a cross section of an input rectangular waveguide is $1\,W$.

For a given excitation (m fixed), expressions (18) allow equivalent voltages and currents $\left(W_1^{(i\pm)}, \ldots, W_N^{(i\pm)}, Y_1^{(i\pm)}, \ldots, Y_N^{(i\pm)}\right)_m$ associated with modes to be obtained. Initial conditions for ordinary differential equations (27) are given by field continuity relations (19a):

$$\forall n \in [0, N-1], \quad (V_n(z=0))_m = \left(V_n^{(i)}\right)_m = \left(W_n^{(i+)} + W_n^{(i-)}\right)_m \quad (I_n(z=0))_m = \left(I_n^{(i)}\right)_m = \left(Y_n^{(i+)} + Y_n^{(i-)}\right)_m \tag{32}$$

For m fixed, final vector $\left(V_1^{(o)}, \ldots, V_N^{(o)}, I_1^{(o)}, \ldots, I_N^{(o)}\right)_m$ is the result of numerical integration of ODEs (27) from $z = 0$ to $z = l$. Output normalized amplitudes are deduced from (18) and (19b) as follows:

$$\forall n \in [1, N], \quad \left(A_n^{(o)}\right)_m = \frac{1}{2\sqrt{Z_n^{(o)}}}\left(\frac{a^{(o)}}{a^{(i)}}\left(V_n^{(o)}\right)_m - Z_n^{(o)}\left(I_n^{(o)}\right)_m\right)$$
$$\left(B_n^{(o)}\right)_m = \frac{1}{2\sqrt{Z_n^{(o)}}}\left(\frac{a^{(o)}}{a^{(i)}}\left(V_n^{(o)}\right)_m + Z_n^{(o)}\left(I_n^{(o)}\right)_m\right)$$
$$V_n^{(o)} = V_n\ (z = l); \quad I_n^{(o)} = I_n\ (z = l) \tag{33}$$

Second, we consider initial independent vector (34): For a propagating mode:

$$\forall n, m \in [1, N], \quad \left(A_n^{(i)}\right)_{m+N} = 0; \quad \left(B_n^{(i)}\right)_{m+N} = K_n \delta_{n,m}; \quad \left(P_n^{(i)}\right)_{m+N} = -\delta_{n,m} \tag{34a}$$

For an evanescent mode:

$$\forall n, m \in [1, N], \quad \left(A_n^{(i)}\right)_{m+N} = -jK_n\delta_{n,m}; \quad \left(B_n^{(i)}\right)_{m+N} = \frac{1}{2}\delta_{n,m}; \quad \left(P_n^{(i)}\right)_{m+N} = -\delta_{n,m} \tag{34b}$$

In accordance with (32), $\left(A_1^{(i)}, A_2^{(i)}, \ldots, A_N^{(i)},\, B_1^{(i)}, B_2^{(i)}, \ldots, B_N^{(i)}\right)_{m+N}$ lead to equivalent currents and voltages that satisfy (35):

$$\forall m \in [1; N], \quad \left(V_1^{(i)}, \ldots, V_N^{(i)},\, I_1^{(i)}, \ldots, I_N^{(i)}\right)_{m+N} = \left(V_1^{(i)}, \ldots, V_N^{(i)},\, -I_1^{(i)}, \ldots, -I_N^{(i)}\right)_m^* \tag{35}$$

Pairs (V_n, I_n) and $(V_n^*, -I_n^*)$ fulfill the same system (27). Therefore, the definition of $2N$ output independent vectors associated with $2N$ input independent vectors given by (31) and (34) requires only N numerical integrations. This method allows the multimodal transmission matrix $[T]$ to be obtained (36). The generalized scattering matrix $[S]$ is deduced from $[T]$ (37). $S_{1,1}^{(ii)}$ is the reflection coefficient of the fundamental mode and $S_{1,1}^{(oi)}$ the transmission coefficient.

$$[T] = \begin{bmatrix} \left(A_1^{(o)}\right)_1 & \left(A_1^{(o)}\right)_2 & \cdots & \left(A_1^{(o)}\right)_{2N} \\ \vdots & \vdots & \ddots & \vdots \\ \left(A_N^{(o)}\right)_1 & \left(A_N^{(o)}\right)_2 & \cdots & \left(A_N^{(o)}\right)_{2N} \\ \left(B_1^{(o)}\right)_1 & \left(B_1^{(o)}\right)_2 & \cdots & \left(B_1^{(o)}\right)_{2N} \\ \vdots & \vdots & \ddots & \vdots \\ \left(B_N^{(o)}\right)_1 & \left(B_N^{(o)}\right)_2 & \cdots & \left(B_N^{(o)}\right)_{2N} \end{bmatrix} \cdot \begin{bmatrix} \left(A_1^{(i)}\right)_1 & \left(A_1^{(i)}\right)_2 & \cdots & \left(A_1^{(i)}\right)_{2N} \\ \vdots & \vdots & \ddots & \vdots \\ \left(A_N^{(i)}\right)_1 & \left(A_N^{(i)}\right)_2 & \cdots & \left(A_N^{(i)}\right)_{2N} \\ \left(B_1^{(i)}\right)_1 & \left(B_1^{(i)}\right)_2 & \cdots & \left(B_1^{(i)}\right)_{2N} \\ \vdots & \vdots & \ddots & \vdots \\ \left(B_N^{(i)}\right)_1 & \left(B_N^{(i)}\right)_2 & \cdots & \left(B_N^{(i)}\right)_{2N} \end{bmatrix}^{-1} \tag{36}$$

$$\begin{pmatrix} B_1^{(i)} \\ \vdots \\ B_N^{(i)} \\ A_1^{(o)} \\ \vdots \\ A_N^{(o)} \end{pmatrix} = [S] \begin{pmatrix} A_0^{(i)} \\ \vdots \\ A_N^{(i)} \\ B_1^{(o)} \\ \vdots \\ B_N^{(o)} \end{pmatrix} \quad \text{and} \quad [S] = \begin{bmatrix} \left[S^{(ii)}\right] & \left[S^{(io)}\right] \\ \left[S^{(oi)}\right] & \left[S^{(oo)}\right] \end{bmatrix} \tag{37}$$

4. NUMERICAL RESULTS

4.1 Restrictions of Numerical Nature

The propagation constant inside the microwave element are unknown. As a result of this lack, the amplitude unknowns $(V_1(z), \ldots, V_N(z), I_1(z), \ldots, I_N(z))$ should be considered as the sum of outgoing waves and incoming waves [13, 14]. The amplitudes first values of these different waves are fixed by initial conditions. A Runge Kutta algorithm is used for solving the initial value problem (27). With such an algorithm, some amplitudes associated with increasing exponential solutions are small instead of being zero [13, Chap. 15 of 14]. This unwanted other solution can be important to consider with the true one. For a long enough transition, sooner or later it dominates. The accuracy in scattering parameters $S_{ij}^{(gg')}((g;g') \in (i;o))$ can be modified. It's essential to overcome this problem especially when the length discontinuity and the excitation vector size are important. For this, we consider the transition as several elementary sections in series. The combination of elementary multimodal scattering matrices by an iteration process already described [15] gives the overall S-matrix of the structure under consideration. The accuracy in parameters $S_{ij}^{(gg')}$ depends on the truncation order N and stub number N_t.

N should be larger than the number of propagative modes TE_{n0} in access rectangular waveguides. N increases with the cross section size. Moreover, in the neighbourhood of junction planes $z = 0$ and $z = l$ and inside the structure, evanescent modes ensure the coupling between outgoing and incoming propagating modes. The accuracy in parameters $S_{ij}^{(gg')}$ depends on the quality of coupling analysis and thus, on the number of evanescent modes taken into account. This number is all the more important since the discontinuity is steep.

From a numerical point of view, one should be capable of fixing the maximum length of the elementary stub knowing the mode number N. We choose the empirical rule presented by E. Marcelin in [5, Ch. 6] that is expressed in this manner: "As soon as the length of the structure under consideration is greater than the quantity proportional to the decaying factor of the Nth evanescent mode, we can not obtain good results any more".

$$l_{\max} \leq K\lambda_N = \frac{2\pi K}{\left|\sqrt{\left(\frac{N\pi}{\min(h(z))}\right)^2 - k^2}\right|} \approx \frac{2K\min(h(z))}{N} \quad \text{for } N \text{ important.} \tag{38}$$

From our numerical experience, $K = 2$ is acceptable. So, we derive the number N_t of elementary transitions by (39) where $\mathrm{Ent}(d)$ denotes the integer part of d and $\min(h(z))$ the minimum of $h(z)$:

$$N_t = \mathrm{Ent}\left(\frac{l}{K\lambda_N}\right) + 1 \approx \mathrm{Ent}\left(\frac{lN}{2K\min(h(z))}\right) + 1 \quad \text{for } N \text{ important.} \tag{39}$$

N_t increases with the structure length l and with the excitation vector size $2N$.

4.2 Analysis of a Sinusoidal Profile Filter

Results presented in Subsections 4.2 and 4.3 are provided using MATLAB on a Pentium II (350 MHz).

The sinusoidal profile structure of Figure 2a can be depicted by the set of 2 transitions symmetrical in relation to $z = l/2$. The scattering matrix $[S_{II}]$ is derived of $[S_I]$ by the inversion of normalized amplitude coefficients $A_n^{(g)}$ and $B_n^{(g)}$. The $[S_I]$ knowledge leads easily to $[S_{II}]$ and by combination [15] to the overall S-matrix of the structure. This discontinuity has also the symmetry plane $x = \frac{a^{(i)}}{2}$. Thus, only odd modes $TE_{2n+1,0}$ are excited.

We consider the transition I of length $l/2$ as N_t elementary sections in series. The accuracy in parameters $S_{ij}^{(gg')}$ depends on N_t. To illustrate this purpose, a measure of error [10] is defined as follows:

With N fixed, $\Delta Q_{ij}^{(gg')}(N_t) = -\log_{10}\left\{\left|\dfrac{S_{ij}^{(gg')}(N_t+1) - S_{ij}^{(gg')}(N_t)}{S_{ij}^{(gg')}(N_t)}\right|\right\}$ (40a)

With N fixed, the quantity $\Delta Q_{ij}^{(gg')}(N_t)$ gives the number of unchanged digits in the coefficient $S_{ij}^{(gg')}$ when N_t is changed into N_t+1. (For example, if $S_{ij}^{(gg')}(N_t) = 0.05$ and $\Delta Q_{ij}^{(gg')} \geq 1$, so $0.045 \leq S_{ij}^{(gg')}(N_t+1) \leq 0.055$ and $-26.9 \leq \left|S_{ij}^{(gg')}(N_t+1)\right|_{dB} \leq 25.2$). Of course, numerical stability is ensured if $\Delta Q_{ij}^{(gg')}(N_t)$ increases with N_t.

Figure 2b gives the accuracy $\Delta Q_{1,5}^{(oi)}(N_t)$ in coefficient $S_{1,5}^{(oi)}$ at 12 GHz for many N values. ($S_{1,5}^{(oi)}$ relates $A_1^{(i)}$ to $B_5^{(o)}$. $A_1^{(i)}$ is associated with the incident mode TE_{10}, $B_5^{(o)}$ to the third transmitted mode $TE_{2n+1,0}$. This mode $TE_{5,0}$ is an evanescent one). Whatever the truncation order N, $\Delta Q_{1,5}^{(oi)}(N_t)$ increases with N_t. This process of elementary S-matrix combination is then efficient. Nevertheless, in accordance with the rule (39), the number $N_{t,\lim}$ of stubs from which some accuracy $\Delta Q_{1,5}^{(oi)}(N_t)$ is ensured increases with N. In other words, $N_{t,\lim}$ increases with the excitation vector size. For example, to obtain $\Delta Q_{1,5}^{(oi)}(N_t) > 4$, we'll have to take $N_t \geq N_{t,\lim} = 8$, 13, and 18 for $N = 5$, 10, and 15, respectively.

We can study the stability of results according to the number of modes $TE_{2n+1,0}$. For this, we define the quantity $\Delta P_{ij}^{(gg')}(N)$ that gives the number of unchanged digits in the coefficient $S_{ij}^{(gg')}$ when N is changed into $N+1$.

With N_t fixed by (39),

$$\Delta P_{ij}^{(gg')}(N) = -\log_{10}\left\{\left|\frac{S_{ij}^{(gg')}(N+1) - S_{ij}^{(gg')}(N)}{S_{ij}^{(gg')}(N)}\right|\right\} \quad (40b)$$

Figure 2c gives the accuracy $\Delta P_{1,5}^{(oi)}(N)$, $\Delta P_{1,1}^{(oi)}(N)$, and $\Delta P_{1,1}^{(ii)}(N)$ in $S_{1,5}^{(oi)}$, $S_{1,1}^{(oi)}$, and $S_{1,1}^{(ii)}$, respectively. Quantities $\Delta P_{ij}^{(gg')}(N)$ in-

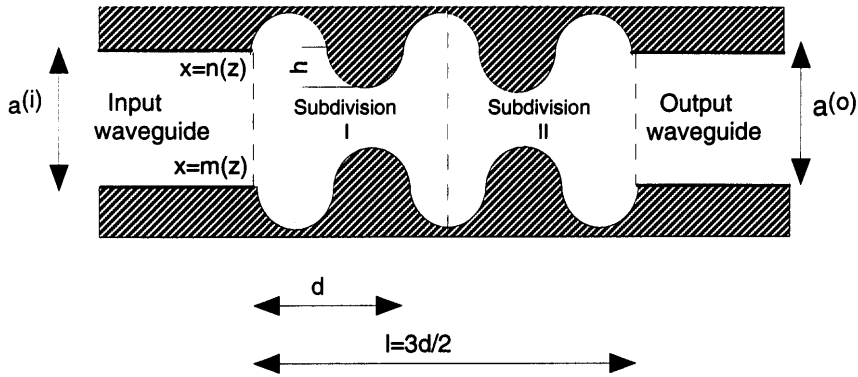

Figure 2a. Sinusoidal profile filter. $m(z) = a^{(i)} + h\sin\left(\frac{2\pi z}{d}\right)$, $n(z) = -h\sin\left(\frac{2\pi z}{d}\right)$, $l = 62.5\,\mathrm{mm}$, $d = 25\,\mathrm{mm}$, $h = 3.5\,\mathrm{mm}$, $a^{(i)} = a^{(o)} = 2b = 19.05\,\mathrm{mm}$.

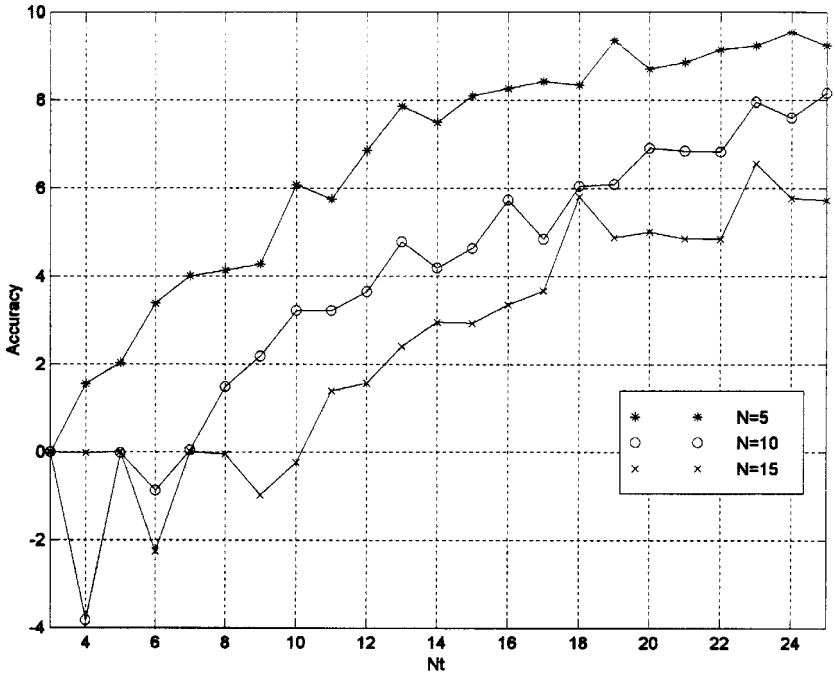

Figure 2b. Accuracy $\Delta Q_{1,5}^{(oi)}(N_t)$ in the transmitted coefficient $S_{1,5}^{(oi)}$ versus stub number N_t for the structure in Figure 2a at $12\,\mathrm{GHz}$ with $N = 5,\ 10,$ and 15.

crease with N. With $N > 14$, the reflected $S_{1,1}^{(ii)}$ and transmitted $S_{1,1}^{(oi)}$ coefficients of the dominant mode are given with 2 correct digits. The same accuracy in $S_{1,5}^{(oi)}$ is obtained from $N = 17$. Nevertheless, we should not infer that for all the configurations, numerical convergence of the coefficients $S_{1,1}^{(ii)}$ and $S_{1,1}^{(oi)}$ is faster than the one associated with S-parameter related higher modes.

Figure 2d shows magnitudes of $S_{1,1}^{(ii)}$ and $S_{1,1}^{(oi)}$ on the range 10–15 GHz with $N = 18$ and $N = 14$. Agreement between these curves is satisfying. The computation time with 26 frequencies is 40 minutes with $N = 8$ and 124 minutes with $N = 14$, that is to say a ratio of 3.

4.3 Steep Discontinuities and Adapted Sectoral Horn

The structure under consideration is shown in Figure 3a. It consists of a rectangular waveguide of cross section $a^{(i)} \times b$ and two trapezoidal septums of base $d + d_0$, height h and rate h/d_0. The two septums are separated by a distance $l - 2(d + d_0)$. Only the dominant mode TE_{10} can propagate. The structure is symmetrical in relation to $z = l/2$. Consequently, $S_{1,1}^{(ii)}$ and $S_{1,1}^{(oo)}$ should be equal. As before, the structure is depicted by the set of 2 symmetrical transitions.

Figures 3b and 3c give the real part and the imaginary part of $S_{1,1}^{(ii)}$ on the range 8–16 GHz with d_0 values smaller and smaller. With $d_0 = d/20$ and $d_0 = d/50$, values of coefficients $S_{1,1}^{(ii)}$ have very weak differences and the comparison with results proposed by Amari et al. in [11, figure 4] is conclusive. Figure 3d gives phase of $S_{1,1}^{(ii)}$, $S_{1,1}^{(oi)}$, $S_{1,1}^{(io)}$, and $S_{1,1}^{(oo)}$. The reciprocity principle is checked $\left(S_{1,1}^{(oi)} = S_{1,1}^{(io)}\right)$ and the symmetry well analyzed $\left(S_{1,1}^{(ii)} = S_{1,1}^{(oo)}\right)$. Our method therefore allows steep discontinuities to be analyzed.

We take 14 modes TE_{n0} to obtain these results. According to the rule (39), the structure is considered as 5 elementary sections in series on $[0; l/2]$. With $d_0 = d/50$ and 17 frequencies, the computation time is 43 minutes.

Figure 4 shows $S_{1,1}^{(ii)}$ magnitude of an adapted sectoral horn on the range 10–15 GHz. This horn consists of a non-linear transition with $l = 50\,\text{mm}$, $a^{(i)} = 2b = 19.05\,\text{mm}$, and $a^{(o)} = 38.10\,\text{mm}$. It has a longitudinal symmetry. We take 8 modes $TE_{2n+1,0}$ for describing the electric and magnetic fields. According to (39), we take 12 elementary

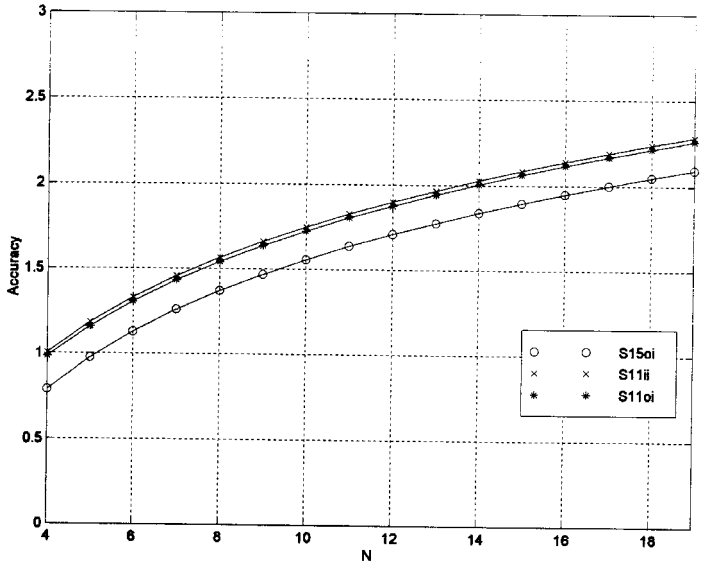

Figure 2c. Accuracies $\Delta P_{1,5}^{(oi)}(N)$, $\Delta P_{1,1}^{(oi)}(N)$, and $\Delta P_{1,1}^{(ii)}(N)$ in coefficients $S_{1,5}^{(oi)}$, $S_{1,1}^{(oi)}$, and $S_{1,1}^{(ii)}$ versus mode number N for the structure in Figure 2a at $12\,\mathrm{GHz}$.

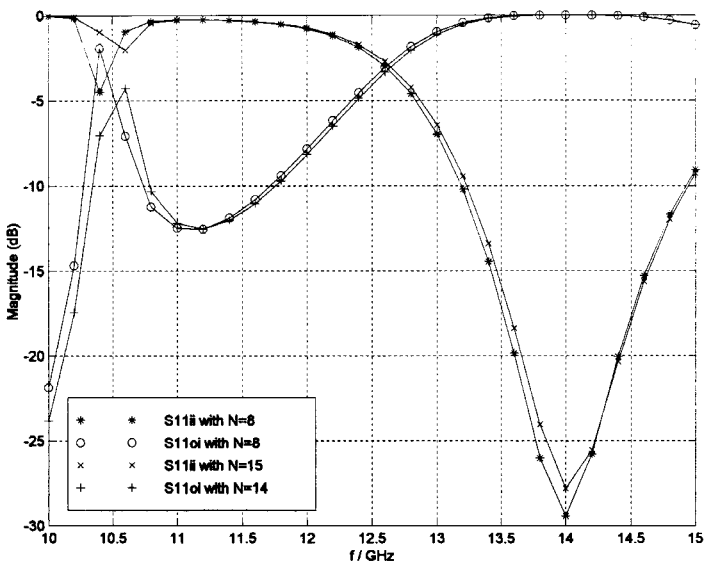

Figure 2d. Magnitude of the reflected coefficient $S_{1,1}^{(ii)}$ and the transmitted coefficient $S_{1,1}^{(oi)}$ versus frequency for the structure in Figure 2a. N_t is given by (39).

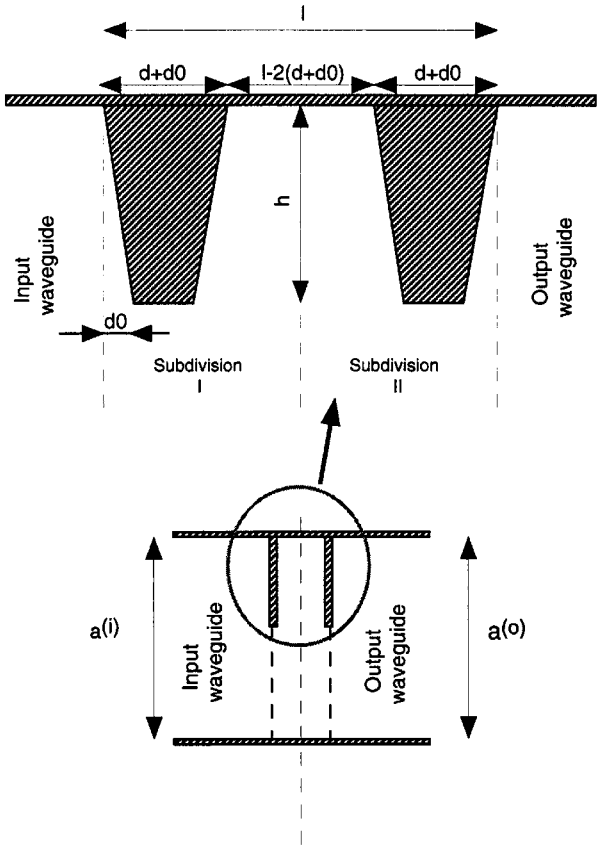

Figure 3a. Structure with two septums. $l = 7\,\mathrm{mm}$, $d = 1\,\mathrm{mm}$, $h = 8.5\,\mathrm{mm}$, $a^{(i)} = a^{(o)} = 2b = 19.5\,\mathrm{mm}$. d_0 is a parameter of the study.

sections. The computation time is 28 minutes with 25 frequencies. The classical modal analysis is used as a reference method [12]. With this method, the horn is approached by a 40-step transformer and the fields described by 8 modes. Agreement between these curves is good.

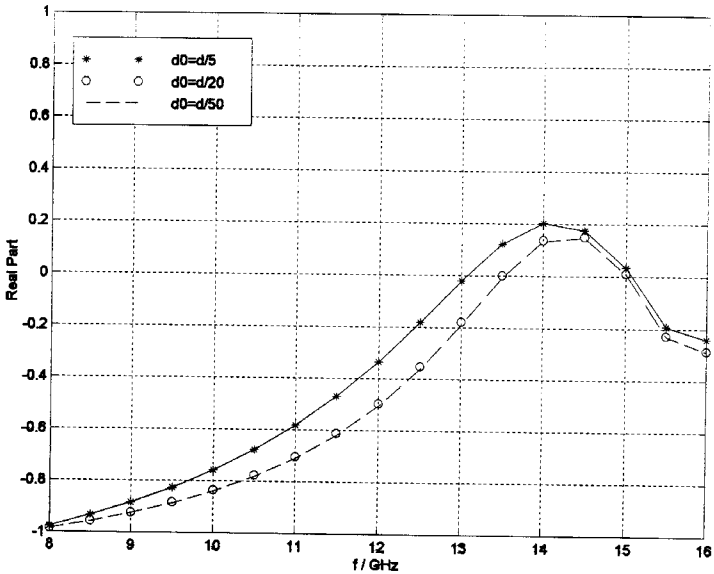

Figure 3b. Real part of the reflected coefficient $S_{1,1}^{(ii)}$ versus frequency for the structure in Figure 3a with $d_0 = d/5$, $d/20$, and $d/50$.

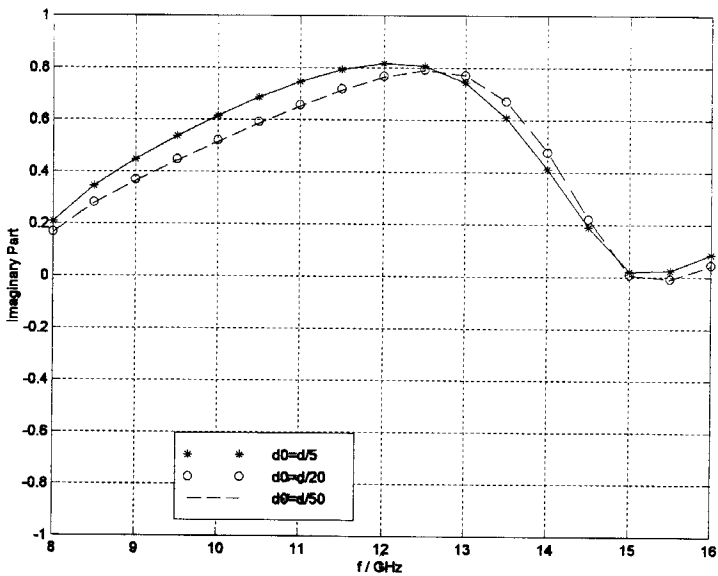

Figure 3c. Imaginary part of the reflected coefficient $S_{1,1}^{(ii)}$ versus frequency for the structure in Figure 3a with $d_0 = d/5$, $d/20$, and $d/50$.

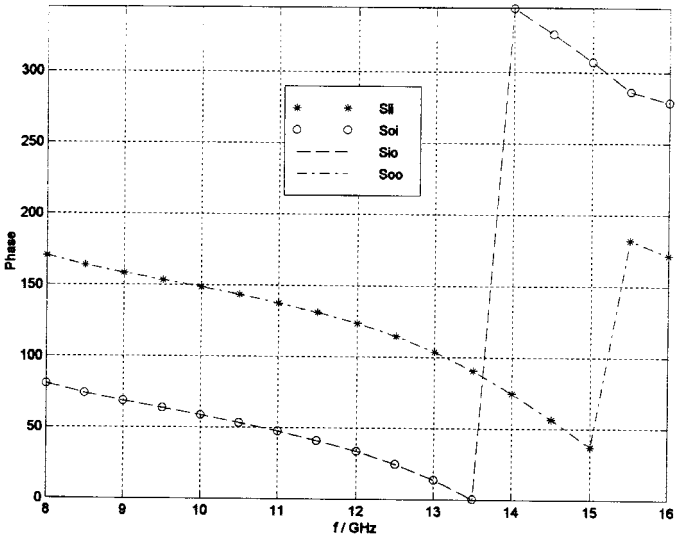

Figure 3d. Phase of $S_{1,1}^{(ii)}$, $S_{1,1}^{(oi)}$, $S_{1,1}^{(io)}$, and $S_{1,1}^{(oo)}$ versus frequency for the structure in Figure 3a with $d_0 = d/50$.

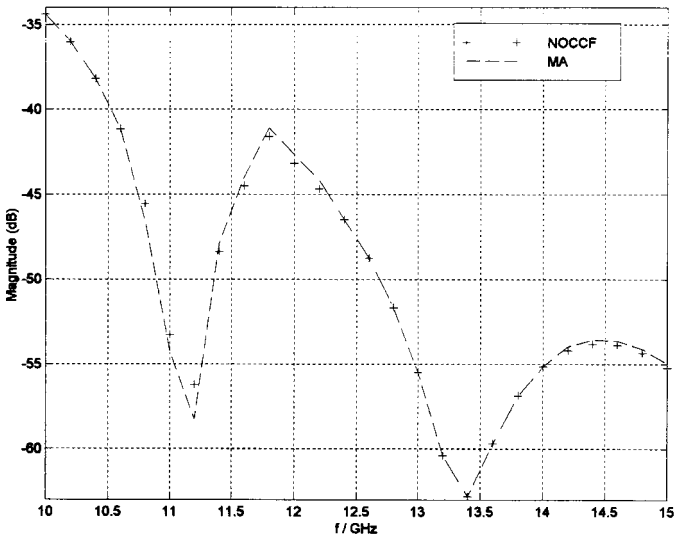

Figure 4. Magnitude of the reflected coefficient $S_{1,1}^{(ii)}$ versus frequency for a non-linear sectoral adapted horn. $m(z) = a^{(i)} - n(z)$, $n(z) = -0.1z - 3.61z^2$, $l = 50\,\text{mm}$, $a^{(i)} = 2b = 19.05\,\text{mm}$, $a^{(o)} = 38.10\,\text{mm}$. Letters MA denote the Modal Analysis, letters NOCCF, the NonOrthogonal Curvilinear Coordinates Formalism.

5. CONCLUSION

The formalism proposed relies on the Maxwell equations written in a nonorthogonal coordinate system fitted to the analyzed H-plane structure geometry. To obtain the generalized S-matrix, this method requires the solving of initial value problem and many numerical integrations with a Runge Kutta algorithm.

During these integrations, unwanted solutions appear which can be important to consider with the true ones. It is essential to overcome this problem especially when the length discontinuity and the TE_{n0} modes number are important. For this, we consider the transition as several elementary sections in series. The combination of elementary multimodal scattering matrices by an iteration process [15] gives the overall S-matrix of the structure under consideration. This process ensures the stability of results.

For compact structures (length and width smaller than $2\text{–}3\,\lambda$), the computation time (mainly due to the integration method and its consequences) is weak enough. Thus, we propose using this analysis tool for shape optimization problems, for example, the design of broad-band filter.

REFERENCES

1. Lewin, L., *Theory of Waveguides.,* Newness-Butterworth, London, 1975.
2. Stratton, J. A., *Electromagnetic Theory,* McGraw-Hill, New York, 1941.
3. Chandezon, J., "Les équations de Maxwell sous forme covariante — Application à l'étude de la propagation dans les guides périodiques et à la diffraction par les réseaux," Thèse d'état, Université Blaise Pascal, Clermont-Ferrand, France, 1979.
4. Chandezon, J. and G. Cornet, "Application d'une nouvelle méthode de résolution des équations de Maxwell à l'étude de la propagation des ondes électromagnétiques dans les guides périodiques," *Ann. Télécom.,* 36, No. 5–6, 305–314, 1981.
5. Marcelin, E., "Application des équations de Maxwell covariantes à l'étude de la propagation dans les guides d'ondes coudés," Thèse d'Université, Université Blaise Pascal, Clermont-Ferrand, France, 1992.
6. Marcelin, E., R. Dusséaux, P. Chambelin, and T. Dusseux, "Forme tensorielle des équations de Maxwell et optimisation de discontinuités plan-H," *12ème Colloque OHD*, 1B1–1B4, Paris,

France, Sept. 1993.

7. Cornet, P., R. Dusséaux, and J. Chandezon, "Wave propagation in curved waveguides of rectangular cross section," *IEEE Trans. Microwave Theory Tech.,* Vol. MTT 47, 965–972, July 1999.
8. Chambelin, P., "Application des équations de Maxwell sous leur forme covariante à l'étude d'antennes cornets rectangulaires," Thèse d'Université, Université Blaise Pascal, Clermont-Ferrand, France, 1995.
9. Chambelin, P., T. Dusseux, R. Dusséaux, and J. Chandezon, "Analysis and synthesis of non-uniform waveguide by tensorial form of Maxwell's equations," *IEEE Ant. and Prop. Symp.,* 1320–1322, Newport Beach, USA, June 1995.
10. Dusséaux R., P. Cornet, and P. Chambelin, "Etude de transformateurs plan-E dans un système de coordonnées non-orthogonal," *Ann. Télécom.,* 54, No. 5–6, Mai–Juin 1999.
11. Amari, S., J. Bornemann, and R. Vahldick, "Accurate analysis of scattering from multiple wavaguide discontinuities using the coupled-integral equations technique," *Journal Elect. Waves Appl.,* Vol. 10, No. 12, 1623–1644, Oct. 1996.
12. Wexler, A., "Solution of waveguide discontinuities by modal analysis," *IEEE Trans. Microwave Theory Tech.,* Vol. MTT. 15, 508–517, Feb. 1967.
13. Huting, W. A. and K. Webb, "Comparison of modes-matching and differential equations techniques in the analysis of waveguide transitions," *IEEE Trans. Microwave Theory Tech.,* Vol. MTT 39, 280–286, Feb. 1991.
14. Press, W. H., B. P. Flannery, S. A. Teukolsky, and W. T. Vetterling, *Numerical Recipes, The Art of Scientific Computing,* Cambridge University Press, Cambridge, 1989.
15. Patzelt, H. and F. Arndt, "Double-plane steps in rectangular wave-guides and their application for transformers, irises and filters," *IEEE Trans. Microwave Theory Tech.,* Vol. MTT 20, 771–776, May 1982.